AR12 (OSU-03012) suppresses GRP78 expression and inhibits SARS-CoV-2 replication

Jonathan O. Rayner [a], Rosemary A. Roberts [a], Jin Kim [a], Andrew Poklepovic [d], Jane L. Roberts [c], Laurence Booth [b], Paul Dent [b,*]

[a] *Department of Microbiology and Immunology, Laboratory of Infectious Diseases, University of South Alabama, Mobile, AL 36688-0002, United States*
[b] *Departments of Biochemistry and Molecular Biology, Virginia Commonwealth University, Richmond, VA 23298-0035, United States*
[c] *Departments of Pharmacology and Toxicology, Virginia Commonwealth University, Richmond, VA 23298-0035, United States*
[d] *Departments of Medicine, Virginia Commonwealth University, Richmond, VA 23298-0035, United States*

ARTICLE INFO

ABSTRACT

AR12 is a derivative of celecoxib which no-longer acts against COX2 but instead inhibits the ATPase activity of multiple chaperone proteins, in particular GRP78. GRP78 acts as a sensor of endoplasmic reticulum stress and is an essential chaperone required for the life cycle of all mammalian viruses. We and others previously demonstrated in vitro and in vivo that AR12 increases autophagosome formation and autophagic flux, enhances virus protein degradation, preventing virus reproduction, and prolonging the survival of infected animals. In this report, we determined whether AR12 could act against SARS-CoV-2. In a dose-dependent fashion AR12 inhibited SARS-CoV-2 spike protein expression in transfected or infected cells. AR12 suppressed the production of infectious virions via autophagosome formation, which was also associated with degradation of GRP78. After AR12 exposure, the colocalization of GRP78 with spike protein was reduced. Knock down of eIF2α prevented AR12-induced spike degradation and knock down of Beclin1 or ATG5 caused the spike protein to localize in LAMP2+ vesicles without apparent degradation. HCT116 cells expressing ATG16L1 T300, found in the majority of persons of non-European descent, particularly from Africa, expressed greater amounts of GRP78 and SARS-CoV-2 receptor angiotensin converting enzyme 2 compared to ATG16L1 A300, predominantly found in Europeans, suggestive that ATG16L1 T300 expression may be associated with a greater ability to be infected and to reproduce SARS-CoV-2. In conclusion, our findings demonstrate that AR12 represents a clinically relevant antiviral drug for the treatment of SARS-CoV-2.

1. Introduction

The chaperone GRP78 / BiP / HSPA5 / Dna K is conserved throughout evolution down to prokaryotes [1,2]. AR12 (OSU-03012) was shown to reduce expression of the chaperone GRP78 through a process requiring autophagosome formation [3]. Subsequently, using quantitative immunofluorescent staining of single cells we determined that AR12 rapidly caused epitopes at the NH2-termini of GRP78, HSP90 and HSP70 to become occluded, whereas epitopes at the COOH-termini were unaffected [4–9]. AR12 was then shown to inhibit the ATPase activities of GRP78, HSP90 and HSP70 with IC50 values in the clinically

relevant 100–300 nM range [9]. In the clinic, AR12 was safely dosed in heavily pre-treated cancer patients at 800 mg BID (NCT00978523; ASCO 2013 meeting, http://meetinglibrary.asco.org /content/ 115148–132). The C max of AR12 in plasma after 1 day at the MTD of 800 mg BID was ~2 μM. After 28 days of treatment the C max was ~3 μM with the peak C max in some patients being ~8 μM. Some patients were on this trial with stable disease for up to 9 months without any drug-related toxicities (DLTs).

AR12 exposure rapidly decreased the expression of: NPC1 and TIM1; LAMP1; and NTCP1, receptors for Ebola / Marburg / Hepatitis A, Lassa fever, and Hepatitis B viruses, respectively [4–8]. Clinically achievable

concentrations of AR12 prevented the replication of drug-resistant HIV, Rabies, Junín, Coxsackievirus B4, Ebola, Chikungunya, Mumps, Measles, Rubella, RSV, CMV, and Influenza viruses. In three different animal models, AR12 suppressed the production of infectious virus particles and prolonged animal survival [6,10,11]. The coronavirus SARS-CoV-2 is the causal agent of the 2020 global COVID-19 pandemic. The development of an anti-viral agent that could suppress SARS-CoV-2 reproduction is viewed as a high priority for biomedical researchers. Before we can consider or attempt to reintroduce AR12 back into the clinic, now as an anti-viral agent, we needed to determine whether it would exhibit anti-viral activity against SARS-CoV-2.

2. Materials and methods

2.1. Materials

In Mobile, the USA-WA1 strain of SARS-CoV-2 virus was acquired from BEI resources (Manassas, VA) and used to establish master and working stocks on Vero E6 (African green monkey kidney) cells. Vero E6 cells were acquired from the ATCC (Manassas, VA) and cultured in DMEM (Lonza), supplemented with 10% FBS (Millipore), 1x L-glutamine (Lonza), and 1x penicillin–streptomycin (Lonza). Virus stocks were verified to be free of mycoplasma contamination and infectious virus titers were determined by standard plaque assay on Vero E6 cells. AR12 (OSU-03012), sorafenib tosylate and pazopanib were purchased from Selleck Chem (Houston, TX). In Richmond, Trypsin-EDTA, DMEM, RPMI, penicillin–streptomycin were purchased from GIBCOBRL (GIBCOBRL Life Technologies, Grand Island, NY). Antibody to detect the SARS-CoV-2 spike protein and the plasmid to express the spike protein were from Sino Biological (Wayne, PA). Antibodies to detect Beclin1, ATG5, HSP90, HSP70, ERK2 and GRP78 were from Cell Signaling (Danvers, MA). ACE2, ODC, TMPRSS2-FITC and TMPRSS11D-AF647 antibodies were purchased from Santa Cruz Biotechnology (Dallas, TX). Total ERK2, HSP90, HSP70, GRP78, eIF2 α, P-eIF2 α S51, ATG5, Beclin1, LAMP2, ATG13, P-ATG13 S318 and IDO1 antibodies were from Cell Signaling (Danvers, MA). Anti-PD-L1, PD-L2 and MHCA antibodies were from ABCAM (Cambridge, UK). Molecules to knock down the expression of Beclin1, ATG5 and eIF2 α, and scramble control, were purchased from Qiagen (Hilden, Germany). Female ADOR cells were a kind gift from a non-small cell lung cancer patient who, without any chemotherapeutic intervention, remains disease free five years after surgical removal of the tumor. The cells contain no 'hot-spot'' mutations. HCT116 ATG16L1 T300 and HCT116 ATG16L1 A300 cells were a kind gift from Dr. David L. Boone, Department of Microbiology and Immunology, Indiana University School of Medicine-South Bend, South Bend, IN [12].

2.2. Methods

2.2.1. Determination of antiviral activity and TCID50 values

TCID50 values were calculated by the Reed-Muench method [13]. To assess antiviral activity of AR12, Vero E6 cells were seeded into 96 well tissue culture plates at 1.7×10^4 cells/well and incubated overnight at 37 °C with 5% CO_2. When cells reached >80% confluence (18 to 24 h) the cells were treated with AR12 at the targeted concentration (1 or 2 μM) in viral growth media [DMEM supplemented with 2% FBS, 1x L-glutamine and 0.2% DMSO (Fisher)]. Control wells received viral growth media alone. After 6 h, the cells were challenged with SARS-CoV-2 virus e.g. at a MOI of 0.001 (1.7×10^1 PFU/well) or 0.01 (1.7×10^2 PFU/well) and returned to the incubator at 37 °C with 5% CO_2. Concentration of drug and DMSO remained constant in control and treated wells during challenge and each condition was tested in 4 wells/ plate. At 24- or 48-hours post-infection, culture supernatant from each well was transferred to tubes for storage at -80 °C and cells were fixed by flooding the plates with 10% neutral buffered formalin. After 1 h, the formalin was removed and replaced with sterile PBS prior to immunofluorescence analysis. For therapeutic assessment, assay conditions remained the same except that the cells were infected first then treated with drug at 3-, 6- or 12-hours post-infection.

For TCID50 analysis, culture supernatant from each individual assay well was aliquoted to 3 wells of a 96 well plate containing DMEM supplemented with 2% FBS, 1x penicillin–streptomycin, and 1x L-glutamine. Ten-fold serial dilutions were performed for each sample and 100 μl of each dilution was transferred to the corresponding well of a 96 well tissue culture plate containing Vero E6 cells. After approximately 72 h incubation at 37 °C with 5% CO_2, the wells from each dilution series were scored for the presence of cytopathic effects and the TCID50/ml titer was calculated using the Reed-Muench method.

2.2.2. Assessments of protein expression and protein phosphorylation

In-cell western blotting was performed using the Hermes WiScan wide-field microscope [14,15]. HCT116 cells (ATG16L1 T300 and A300) are sub-cultured into individual 96-well plates. Twenty-four hours after plating, the cells are transfected with a control plasmid or a control siRNA, or with an empty vector plasmid or with a plasmid to express the SARS-CoV-2 spike protein. After another 24 h, the cells are treated with vehicle control or AR12. At various time-points after the initiation of drug exposure, cells are fixed in place using paraformaldehyde and using Triton X100 for permeabilization. Standard immuno-fluorescent blocking procedures are employed, followed by incubation of different wells with a variety of validated primary antibodies and subsequently validated fluorescent-tagged secondary antibodies are added to each well. Of note for scientific rigor is that the operator does not personally manipulate the microscope to examine specific cells; the entire fluorescent accrual method is independent of the operator. The Hermes microscope software randomly assesses the fluorescence intensity of 100 cells per treatment condition generating a mean fluorescence intensity read-out value to the investigator. The experiment is performed two additional times to provide an n = 3 (300 cells randomly analyzed).

2.2.3. Transfection of cells

Cells from a fresh culture growing in log phase were transfected 24 h after plating. Prior to transfection, the medium was aspirated, and serum-free medium was added to each plate. For transfection, 10 nM of the annealed siRNA, scrambled or against eIF2 α, Beclin1 or ATG5 were used. Ten nM siRNA (scrambled or experimental) was diluted in serum-free media. Four μl Hiperfect was added to this mixture and the solution was mixed by pipetting up and down several times. This solution was incubated at room temp for 10 min, then added drop-wise to each dish. The medium in each dish was swirled gently to mix, then incubated at 37 °C for 2 h. Serum-containing medium was added to each plate, and cells were incubated at 37 °C for 24 h before drug treatment.

2.2.4. Assessments of autophagosome and autolysosome levels

Cells were transfected with a plasmid to express LC3-GFP-RFP (Addgene, Watertown MA). Twenty-four h after transfection, cells are treated with vehicle control or AR12 (2 μM). Cells were imaged at 60X magnification 4 h and 8 h after drug exposure and the mean number of GFP+ and RFP+ punctae per cell determined from >50 randomly selected cells per condition.

2.2.5. Quantification of phagocytosis

Phagocytosis was calculated at 15- and 60 min post-addition using flow cytometry analysis as described in Martinez et al. [16]. The percentage of phagocytosis equals the number of macrophages that have been engulfed PKH26-stained apoptotic cells, OVA-Alexa Fluor 594 (Invitrogen #O34783), or Zymosan-Alexa Fluor 594 (Invitrogen #Z23374). Data represent a minimum of 2 independent experiments in which technical triplicates of 50,000 cells per sample were acquired using a Fortessa cytometer (BD).
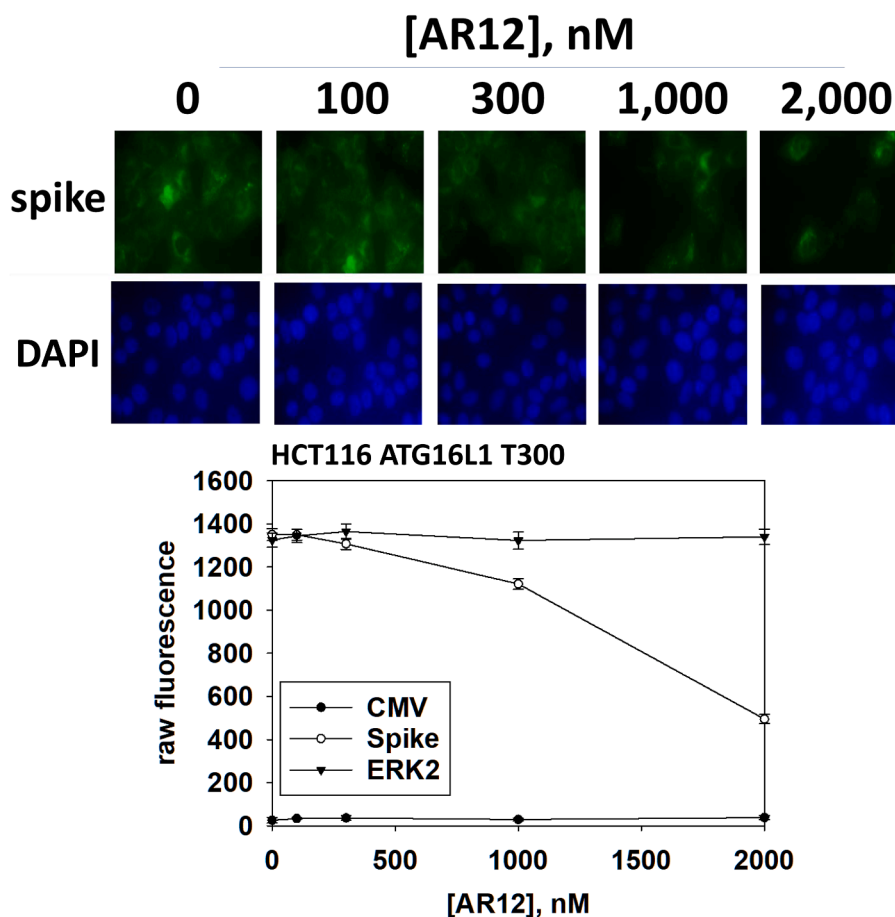
Fig. 1. AR12 reduces SARS-CoV-2 spike protein expression in a dose-dependent fashion. HCT116 ATG16L1 T300 cells were transfected with a plasmid to express the SARS-CoV-2 spike protein. Twenty-four h later, cells were treated with vehicle control or with AR12 (100–2000 nM) for 6 h and fixed. Cells were stained to determine the expression of the SARS-CoV-2 spike protein and for ERK2 as a loading control. (n = 3 ±SD).

2.2.6. Data analysis

Comparison of the effects of various treatments was done using one-way ANOVA and a two tailed Student's *t*-test. Differences with a p-value of < 0.05 were considered statistically significant. Experiments are the means of multiple individual discrete points from multiple experiments (±SD).

3. Results

We initially performed a dose–response curve with AR12, examining its ability to down-regulate the expression of the SARS-CoV-2 spike protein. Cells were transfected to express the spike protein and then treated with increasing concentrations of AR12. In a dose-dependent fashion AR12 reduced spike protein expression without altering the expression of the loading control ERK2 (Fig. 1).

Vero cells were treated with AR12 (1 μM; 2 μM) and then infected with SARS-CoV-2 at 0.01 and 0.001 multiplicities of infection (MOI). Twenty-four and forty-eight hours after infection, cells were fixed in place and permeabilized, and stained for expression of the SARS-CoV-2 spike protein, total GRP78 and total ERK2 as a loading control. In a dose-dependent fashion, AR12 suppressed the production of virus spike protein (Fig. 2A and B). Cells were then infected and treated with AR12 (2 μM) 3 h, 6 h and 12 h after infection, with cells being fixed and stained 24 h after infection. Treatment of infected cells with AR12 significantly reduced the amount of spike protein produced in the infected cells as well as the amount of GRP78 in the cells (Fig. 2C and D).

Vero cells were treated with AR12 (2 μM) and 6 h later infected with SARS-CoV-2 at 10 MOI. Forty minutes after infection, the cells were washed and then fixed in place, and the amount of virus spike protein associated with the Vero cell plasma membrane determined (Fig. 3A). Prior AR12 exposure reduced the amount of virus associated with the Vero cell plasma membrane by >75% (p < 0.05). Prior treatment for 6 h and 10 min with AR12 significantly reduced the total expression of GRP78 (Fig. 3B). AR12 did not or very weakly reduced the expression of ACE2 at the (6 h + 10 min) and (6 h + 40 min) time points, respectively. AR12 did not or very weakly reduced the expression of HSP90 and HSP70 at the (6 h + 10 min) and (6 h + 40 min) time points, respectively. This data implies that AR12, acting both as a direct inhibitor of GRP78 and by causing GRP78 break down, promotes the denaturation and inactivation of the ACE2 receptor; the denatured receptor cannot bind to the SARS-CoV-2 virus. Infection of cells with 0.01 MOI of SARS-CoV-2 caused the total expression of GRP78 to be significantly enhanced, 24 h/48 h after infection, whilst the expression of ERK2 remained constant (Fig. 3C). AR12, in a dose-dependent fashion, significantly reduced basal GRP78 levels and almost abolished virus-stimulated GRP78 expression. Previously, we had also shown the multi-kinase and chaperone inhibitors sorafenib and pazopanib could suppress virus reproduction [7]. However, compared to AR12, neither drug as strongly reduced spike protein nor GRP78 expression (Fig. 4).

GRP78 binds to and keeps inactive PKR-like endoplasmic reticulum kinase (PERK). PERK phosphorylates and inactivates eIF2α; for a virus, increased eIF2α phosphorylation will reduce translation of virus proteins, and our findings that virus infection increases GRP78 expression is concordant with this concept. AR12 increased the inhibitory serine 51 phosphorylation of eIF2α regardless of viral infection (Fig. 5A). Interestingly, virus infection increased the total expression of eIF2α, which
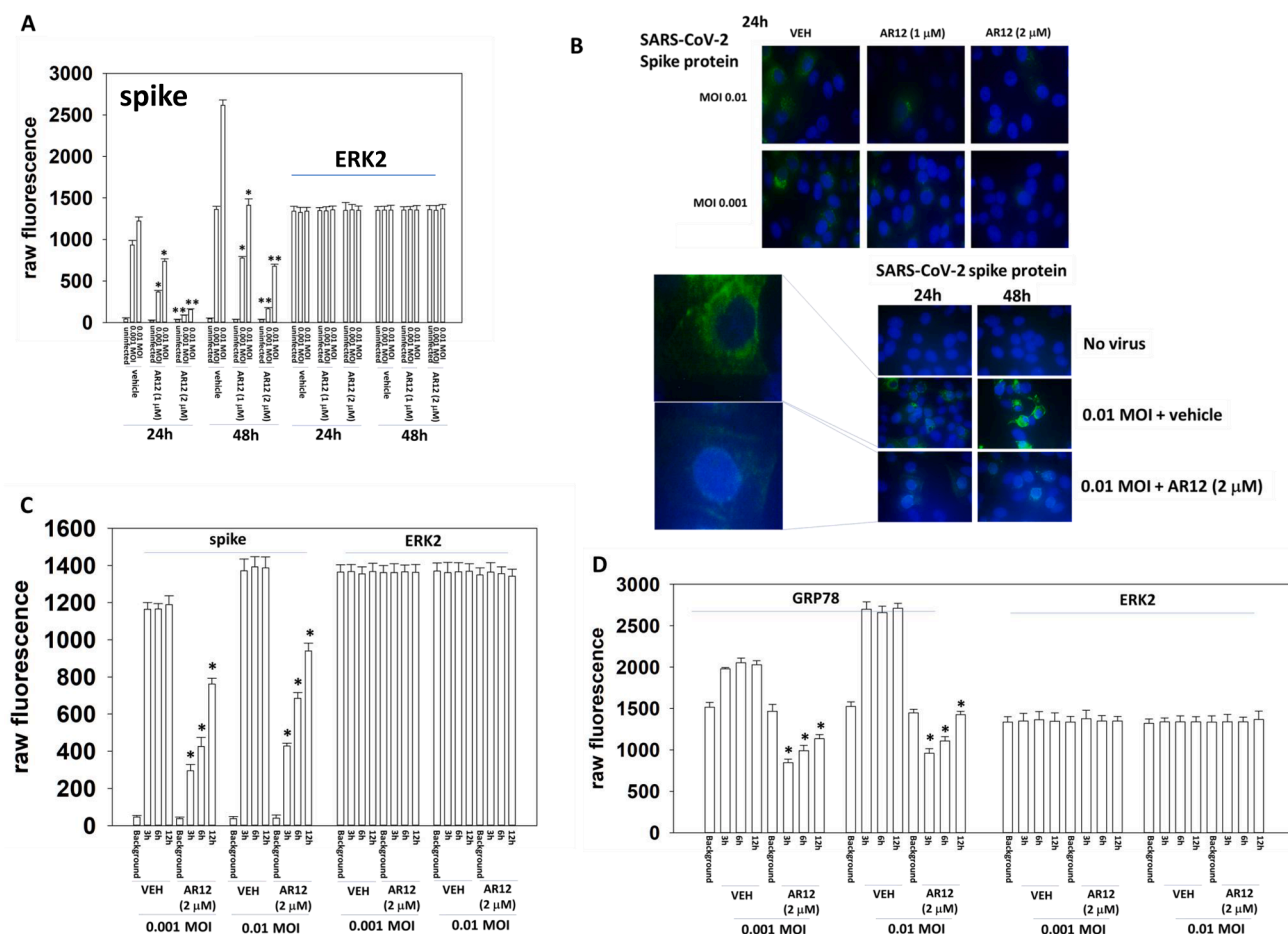
Fig. 2. AR12 suppresses the synthesis of the SARS-CoV-2 spike protein. A. Vero cells were treated with vehicle control or AR12 and 6 h later infected with SARS-CoV-2 as described in the Methods and Figure. Cells were fixed after 24 h or 48 h and the expression of the spike protein determined (n = 2 independent experiments each with 4 independent assessments +/-SD) *p < 0.05 less than corresponding values in vehicle control treated; ** p < 0.05 less than corresponding values in 1 μM AR12 treated cells. B. Representative 60X images of drug-treated cells; blue DAPI = nucleus; green = SARS-CoV-2 spike protein. C. and D. Vero cells were infected with SARS-CoV-2 and then treated with vehicle control or with AR12 (2 μM), 3 h, 6 h and 12 h after infection. All cells were fixed 24 h after infection and the expression of the spike protein and GRP78 determined (n = 2 independent experiments each with 6 independent assessments ±SD) *p < 0.05 less than corresponding values in virus infected cells.

was enhanced by AR12. Knock down of eIF2α prevented AR12 from reducing spike protein expression (Fig. 5B and C). Notably, when expression of eIF2α was knocked down, the spike protein became localized in punctate structures that co-stained for ATG5 (Fig. 5C and D). Although AR12 increased expression of Beclin1, in the absence of eIF2α, AR12 surprisingly reduced Beclin1 levels (Fig. 5C and D). Similar data were also observed for ATG5 (data not shown). The chaperone GRP78 colocalized with the virus spike protein, an interaction disrupted by AR12 (Fig. 6A and B). Under control conditions the spike protein and GRP78 colocalize, and the merged image is yellow. In the presence of AR12, not only is there less spike protein and GRP78 protein, but the colocalization color is now a green shade of yellow, indicating a greater degree of degradation of GRP78 than of the spike protein.

We then determined whether the AR12-dependent effects we had observed on the expression of virus spike protein and on GRP78 levels were associated with reduced production of infectious virus. The supernatants of infected cells, pre-treated with AR12 for 6 h, were isolated 24 h after infection, and the 50% tissue culture infectious dose (TCID$_{50}$) / ml titers determined. In a dose-dependent fashion, AR12 significantly reduced the production of infectious SARS-CoV-2 (Fig. 7A). The data presented are from four independent studies and within each study containing four independent determinations. In parallel, supernatants of infected cells, treated with AR12 6 h after infection, were isolated 24 h after infection, and the TCID$_{50}$/ml titers determined. AR12 significantly

reduced the production of infectious SARS-CoV-2 (Fig. 7B). The data presented are also from four independent studies and within each study containing four independent determinations.

During the COVID-19 pandemic, African-Americans to a greater extent than European-Americans have been infected and killed by SARS-CoV-2. Many environmental and societal factors have been suggested to play causal roles in this epidemiology. One factor we have considered is the differential isoform expression of the autophagy regulatory protein ATG16L1 between African-Americans and European-Americans [17–22]. African-Americans have been found to express ATG16L1 T300 to a greater extent than European-Americans who more frequently express ATG16L1 A300; homozygous expression of ATG16L1 A300 is associated with a greater incidence of Crohn's Disease, due to a reduced ability of immune cells to phagocytose and digest, via autophagy, inflammatory materials in the GI. On the other hand, expression of ATG16L1 T300 has been linked to the greater metastatic spread of tumors [19]. The ability of AR12 to stimulate autophagosome formation and cause autophagic flux was reduced in cells expressing the ATG16L1 A300 isoform (Fig. 8A) [4,6,7]. The ability of AR12 to reduce expression of the SARS-CoV-2 spike protein required autophagosome formation (Fig. 8B). In cells expressing ATG16L1 T300, AR12 significantly reduced spike protein expression by 71% whereas in cells expressing ATG16L1 A300, AR12 only reduced spike protein levels by 16% (p < 0.05). The ability of AR12 to reduce the expression of GRP78, HSP90 and HSP70
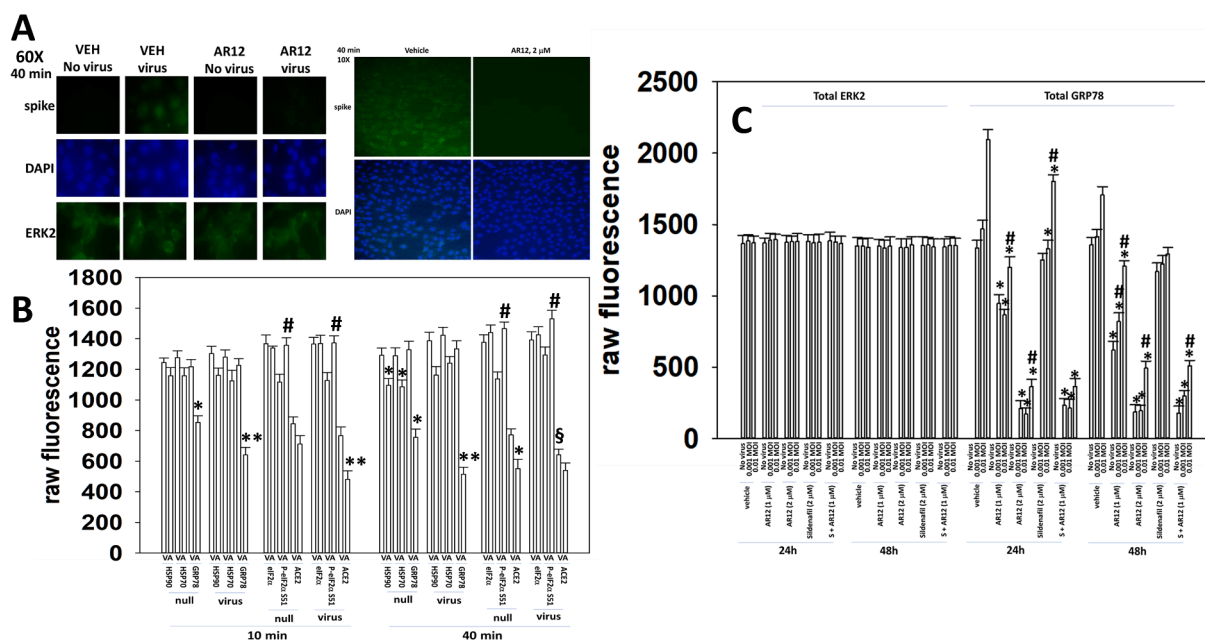
Fig. 3. AR12 suppresses the expression of GRP78 and reduces the increase in GRP78 expression caused by SARS-CoV-2. A. Vero cells were pre-treated with vehicle control or with AR12 for 6 h. Cells were infected with SARS-CoV-2 (10 MOI). Forty minutes after infection, the media was removed, and the cells washed with PBS three times. The cells were fixed in place without permeabilization and cells stained to determine the levels of spike protein on the outer leaflet of the plasma membrane, with DAPI and ERK2 as loading controls. B. Vero cells were pre-treated with vehicle control or with AR12 for 6 h. Cells were then infected (10 MOI). The cells were fixed in place with permeabilization 10 min and 40 min after infection and the total expression of ACE2, GRP78, HSP90, HSP70, eIF2α, P-eIF2α S51 and ERK2 (not shown) determined. (n = 2 independent experiments each with 4 independent assessments ±SD) *p < 0.05 less than corresponding values in vehicle control treated; ** p < 0.05 less than corresponding AR12 value in uninfected cells; § p < 0.05 less than corresponding vehicle value in uninfected cells. C. Vero cells were treated with vehicle control or AR12 (1 μM, 2 μM), sildenafil (2 μM) or the drugs combined and 6 h later infected with SARS-CoV-2 as described in the Methods and the Figure. Cells were fixed after 24 h or 48 h and the expression of GRP78 and ERK2 determined (n = 2 independent experiments each with 4 independent assessments ±SD) *p < 0.05 less than corresponding values in vehicle control treated; # p < 0.05 greater than corresponding value in uninfected cells.
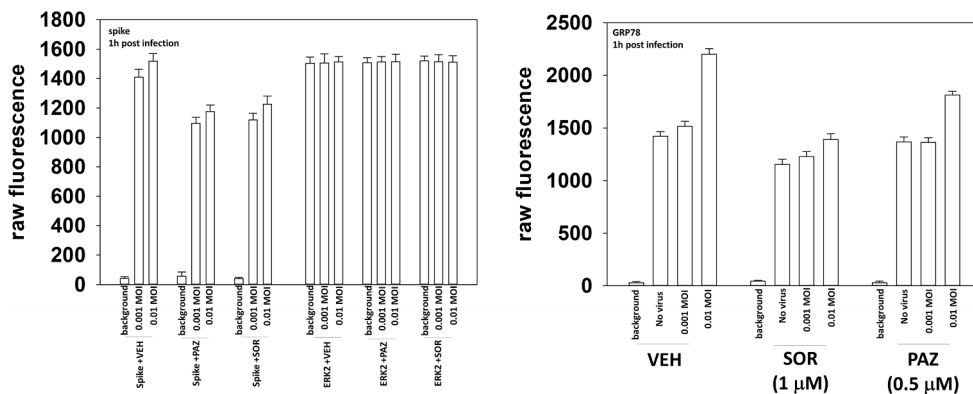
Fig. 4. Sorafenib and pazopanib modestly reduce spike protein and GRP78 expression in SARS-CoV-2 infected cells. Vero cells were infected with the indicated multiplicities of infection with SARS-CoV-2. One hour after infection, cells were treated with vehicle control, sorafenib tosylate (1.0 μM) or pazopanib (0.5 μM). Twenty-four h after infection, cells were fixed in place. Fixed cells were subjected to in-cell western blotting as described in the Methods to determine the expression of the indicated proteins (n = 3 independent studies ±SD).

also required autophagosome formation (Fig. 8C and D).

In vehicle control treated cells, we noted that knock down of either Beclin1 or ATG5, regardless of ATG16L1 isoform expression, altered the sub-cellular localization of the spike protein, from a diffuse mackerel stain to a more punctate form of staining (Fig. 8E, upper). Exploratory studies then determined whether knock down of the autophagosome regulatory proteins caused the spike protein to become localized in endosomes/lysosomes. After knock-down of either ATG5 or Beclin1 in HCT116 ATG16L1 T300 cells, the spike protein under basal conditions co-localized with the endosome marker LAMP2 (Fig. 8E, lower). Treatment of scrambled control cells with AR12 reduced spike expression and caused punctate co-localization of LAMP2 and Beclin1. Knock down of Beclin1 or ATG5 both increased basal levels of LAMP2 by ~25% (p < 0.05). Understanding how knock down of Beclin1 or ATG5 alters the sub-cellular localization of the spike protein into LAMP2+ vesicles will

require studies beyond the scope of the present manuscript.

We compared the plasma membrane / surface (S) levels of the SARS-CoV-2 ACE2 receptor in Vero cells, a PDX non-small cell lung cancer isolate ADOR and HCT116 ATG16L1 T300 cells. The ADOR cells expressed approximately twice the amount of ACE2 compared to Vero cells and the HCT116 cells expressed approximately five times the amount of (Fig. 9A). We then compared the ability of ADOR cells and Vero cells to be infected and produce spike protein in the presence or absence of AR12. Both cells expressed similar amounts of GRP78 and ERK2, and in both cells AR12 reduced GRP78 expression (Fig. 9B). However, ADOR cells, despite being infected with ten-times more virus particles than the Vero cells, modestly expressed the SARS-CoV-2 spike protein. AR12 significantly reduced the total and cell surface levels of GRP78 and ACE2 in ADOR cells whereas AR12 did not reduce the expression of the ACE2 virus receptor in Vero cells (Fig. 9C, not shown).
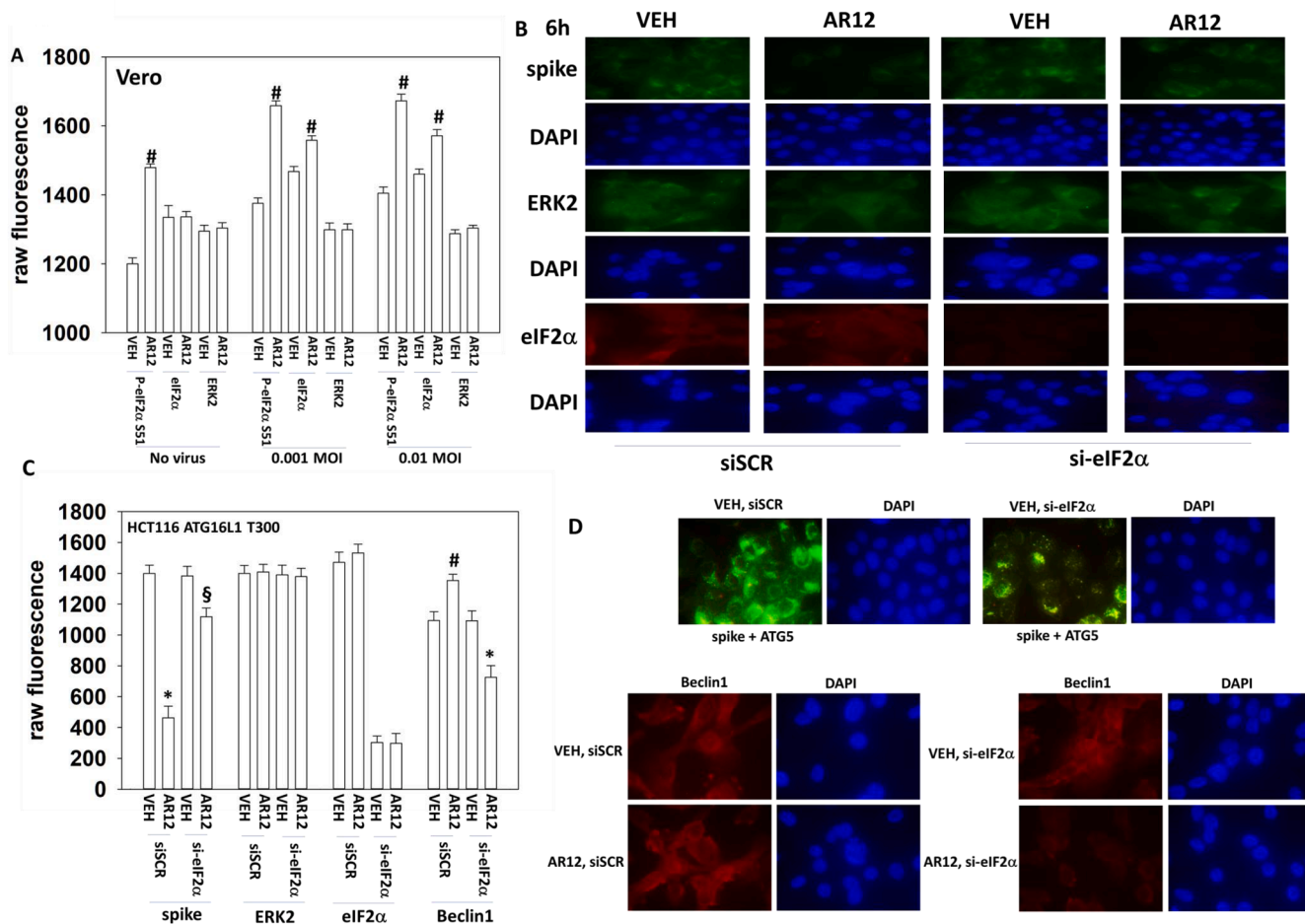
Fig. 5. AR-12 inactivates eIF2α regardless of viral infection. A. Vero cells were treated with vehicle control or AR12 (2 μM) and 6 h later infected with SARS-CoV-2 as described in the Methods. Cells were fixed after 24 h and the expression of eIF2α, phospho-eIF2α serine 51 and ERK2 determined (n = 2 independent experiments each with 4 independent assessments ±SD) # p < 0.05 greater than corresponding value in vehicle control treated cells. B. and C. HCT116 ATG16L1 T300 cells were transfected to express the SARS-CoV-2 spike protein and in parallel, transfected with a scrambled siRNA (siSCR) or an siRNA to knock down the expression of eIF2α. Twenty-four h later, cells were treated with vehicle control or AR12 (2 μM) and 6 h later the cells fixed in place. The expression of spike protein, eIF2α and ERK2 were determined (n = 2 independent experiments each with 3 independent assessments ±SD) * p < 0.05 less than vehicle control value; # p < 0.05 greater than vehicle control value; § p < 0.05 greater than corresponding value in siSCR cells. D. HCT116 ATG16L1 T300 cells were transfected to express the SARS-CoV-2 spike protein and in parallel, transfected with a scrambled siRNA (siSCR) or an siRNA to knock down the expression of eIF2α. Twenty-four h later, cells were treated with vehicle control or AR12 (2 μM) and 6 h later the cells fixed in place. The co-localization of viral spike protein and ATG5 was determined. The expression of Beclin1 was presented pictorially.
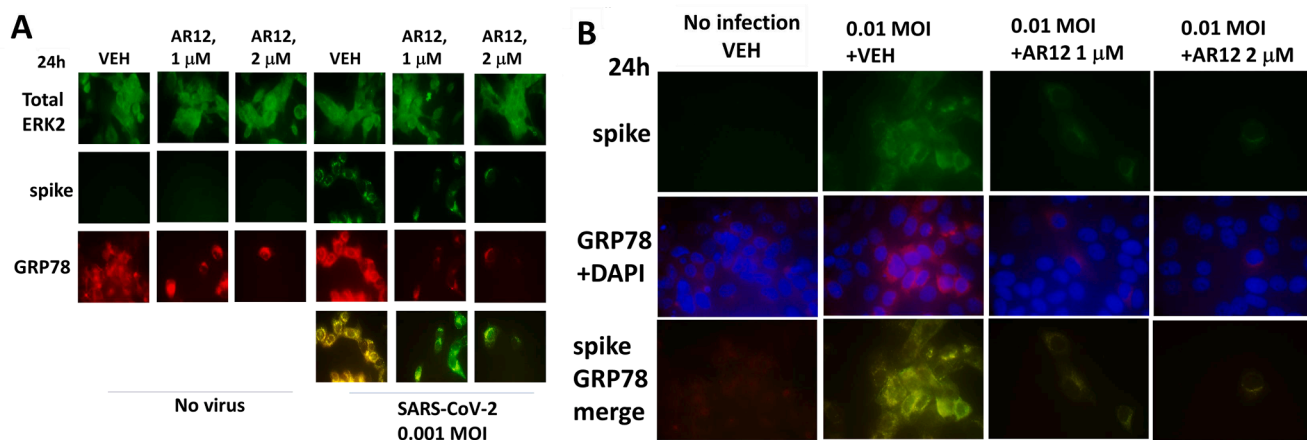
Fig. 6. Representative images of GRP78 and SARS-CoV-2 spike protein expression and co-localization. A. and B. Vero cells were treated with vehicle control or AR12 (1 μM, 2 μM) and 6 h later infected with SARS-CoV-2 as described in the Methods. Cells were fixed after 24 h and the expression of GRP78 and ERK2 determined (n = 2 independent experiments each with 4 independent assessments +/-SD). Representative 60X images at the 24 h timepoint of the colocalization of the virus spike protein (green) and GRP78 (red). DAPI (blue) staining is the nucleus.
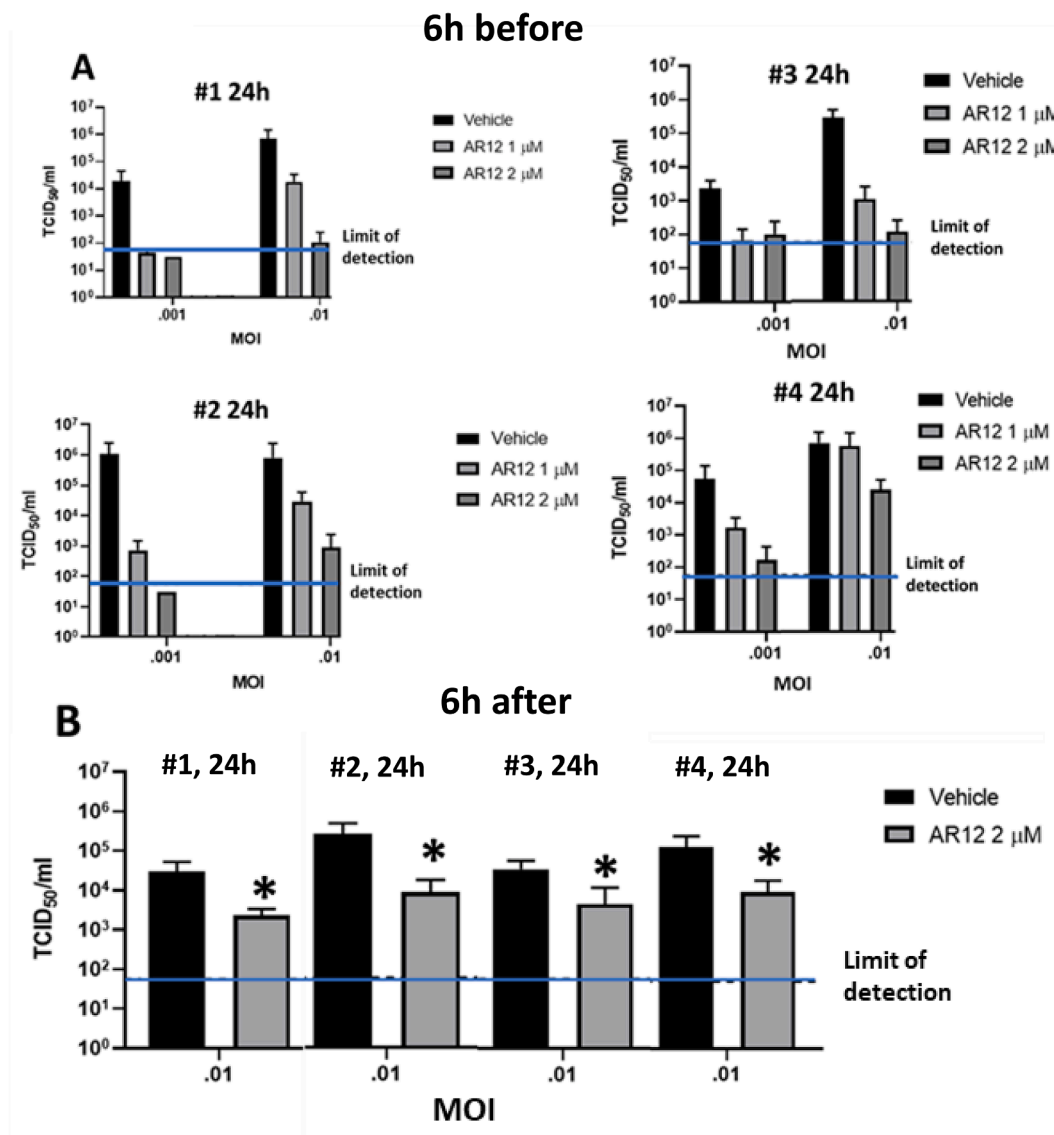
Fig. 7. AR12 suppresses the production of infectious SARS-CoV-2 virions. A. Four independent $TCID_{50}$ / ml studies are presented, each study in independent quadruplicate. Vero cells were *pre-treated* with AR12 and 6 h afterwards infected, and 24 h later the media was removed from the cells. The media was diluted 1:10, with repeated 1:10 dilutions using the Reed-Muench method. B. Four independent $TCID_{50}$ / ml studies are presented, each study in independent quadruplicate. Vero cells were infected then *after* 6 h treated with AR12, and 24 h later the media was removed from the cells. The media was diluted 1:10, with repeated 1:10 dilutions using the Reed-Muench method.

Comparing isogenic matched HCT116 ATG16L1 T300 and HCT116 ATG16L1 A300 cells, we found the expression of cell surface (S) and total expression of GRP78 (T) was reduced by approximately 25% in the HCT116 ATG16L1 A300 cells (Fig. 9D). The expression levels of ACE2 were also approximately 20% lower in the HCT116 ATG16L1 A300 cells. AR12 reduced the expression of GRP78 and ACE2 and increased the phosphorylation of ATG13 S318 and eIF2α S51. However, the ability of AR12 to increase the phosphorylation of ATG13 and eIF2α was significantly lower in the HCT116 ATG16L1 A300 cells. This is in further agreement with the reduced ability of the A300 cells from forming autophagosomes and performing autophagic flux.

Infection of HCT116 cells with SARS-CoV-2 did not induce any obvious cytopathic effect in either the T300 or the A300 cells within 96 h, and as assessed by $TCID_{50}$ / ml assays. ADOR cells were capable of producing modest amounts of infectious virions (Fig. 10A and B). Thus, the levels of ACE2 in a cell do not correlate to the infectivity and viral reproduction capacity of cells. In a similar manner to our prior analyses, we determined whether the SARS-CoV-2 spike protein and the

chaperone GRP78 co-localized in ADOR cells (Fig. 10C). Twenty-four hours after infection, some of the cells exhibited GRP78 and spike protein co-localization, as judged by the cells staining orange. Portions of the cell population remained red, i.e. expressing GRP78 without spike protein. However, in cells expressing the highest levels of spike protein, low levels of GRP78 were present. DAPI staining for cells expressing high levels of spike protein revealed that the nuclear DNA was no-longer contained within an ovoid body, i.e. the cells had been killed by virus infection. Thus, ADOR cells contain at least two distinct populations of cells who respond differentially to SARS-CoV-2.

Our spike protein expression data comparing Vero cells and ADOR cells raised the possibility that the ability of SARS-CoV-2 to enter ADOR cells and HCT116 cells was compromised compared to that found in Vero cells. Trans-membrane serine proteases: serine subfamily member 2 (TMPRSS2) and TMPRSS11D, have been shown to play a key role in cleaving the SARS-CoV S protein at residues R667 and R797 [23]. These proteases played an essential role in the life cycle of the coronavirus SARS-CoV. Subsequently, similar data were obtained for SARS-CoV-2
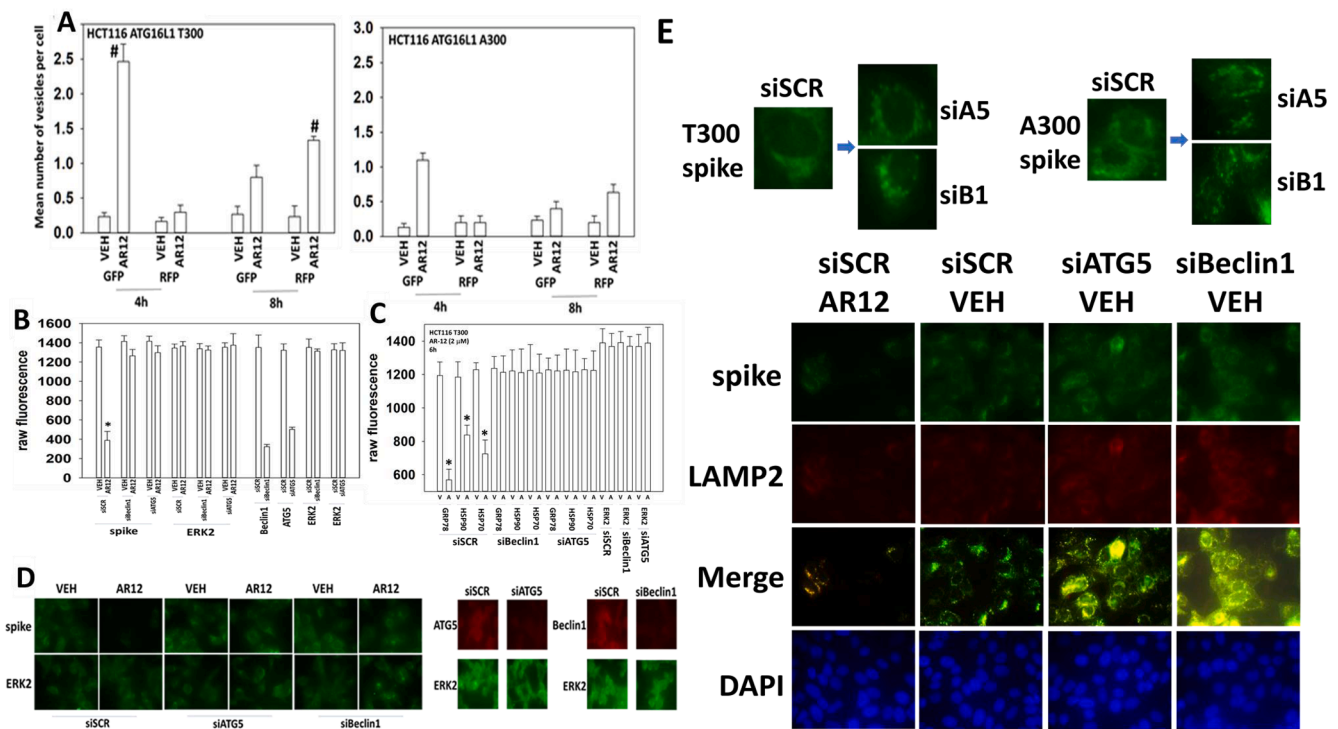
Fig. 8. AR12 reduces the expression of SARS-CoV-2 spike protein, GRP78, HSP90 and HSP70 via autophagy. A. HCT116 cells (ATG16L1 A300 and T300) were transfected with a plasmid to express LC3-GFP-RFP. Twenty-four h after transfection, cells were treated with vehicle control or with AR12 (2 μM). Cells were imaged 4 h and 8 h after drug exposure and the mean number of GFP + and RFP + punctae per cell determined from at least 40 cells per condition (n = 3 ±SD) # p < 0.05 greater than corresponding value in A300 cells. B. HCT116 ATG16L1 T300 cells were transfected with a plasmid to express the SARS-CoV-2 spike protein, and also transfected with a scrambled siRNA or siRNA molecules to knock down the expression of Beclin1 or ATG5. Twenty-four h after transfection, cells were treated with vehicle control or AR12 (2 μM). After a further 6 h incubation, cells were fixed and staining for the spike protein performed (n = 3 ±SD) * p < 0.05 less than corresponding value in siSCR cells. Images of the siRNA knockdown and AR12 spike-suppressive effects are presented in *Panel D* at 60X magnification. C. HCT116 ATG16L1 T300 cells were transfected with a scrambled siRNA or siRNA molecules to knock down the expression of Beclin1 or ATG5. Twenty-four h after transfection, cells were treated with vehicle control or AR12 (2 μM). After a further 6 h incubation, cells were fixed and staining for GRP78, HSP90 and HSP70 performed (n = 3 ±SD) * p < 0.05 less than corresponding value in siSCR cells. E. HCT116 ATG16L1 T300 and A300 cells were transfected with a scrambled siRNA or siRNA molecules to knock down the expression of Beclin1 or ATG5. Twenty-four h after transfection, cells were treated with vehicle control and after 6 h fixed in place. Upper: representative 60X images staining for the SARS-CoV-2 spike protein. Lower: representative 60X images staining for the co-localization of the SARS-CoV-2 spike protein and the endosomal protein LAMP2 in HCT116 ATG16L1 T300 cells.

[24,25]. Compared to Vero cells, ADOR cells and HCT116 cells expressed significantly lower levels of both TMPRSS2 and TMPRSS11D (Fig. 10D). This data implies that the expression levels of S protein serine proteases may represent a better biomarker for SARS-CoV-2 infection and reproduction than the expression of the virus receptor itself, ACE2.

Checkpoint inhibitory immunotherapy antibodies, particularly those that inhibit PD-L1, are a standard of care approach in diseases such as melanoma and non-small cell lung cancer. Treatment of HCT116 ATG16L1 T300 or A300 cells with AR12 modestly reduced the expression of PD-L1 (Fig. 11). In T300, but not A300, cells, AR12 treatment increased expression of class I MHCA, however, ATG16L1 A300 cells expressed higher basal levels of MHCA. Additional studies beyond the scope of the present manuscript will be required to solidify this hypothesis. Prior studies in solid tumor cells, and our present work in ADOR and HCT116 cells demonstrated that AR12 could reduce the level of plasma membrane virus receptors. We determined whether AR12, in immune cells, could enhance the phagocytosis of extracellular antigens. AR12 did not significantly enhance antigen uptake in immune cells, regardless of Rubicon expression (data not shown).

4. Discussion

Our data demonstrates that AR12, in a manner very similar to prior studies, suppresses the ability of SARS-CoV-2 to produce virus spike protein and to generate infectious virions [3–9]. AR12 reduces the expression of cell surface ACE2 and GRP78, as well as total GRP78

levels. We have previously published that AR-12-induced GRP78 degradation is causal in the formation of autophagosomes. Thus, AR12 both catalytically inhibits the GRP78 ATPase activity, reducing its ability to renature proteins in the endoplasmic reticulum, and decreases the protein levels of the chaperone, all of which are associated with lower amounts of spike protein and infectious virus production. These data support the re-entry of AR12 into the clinic as an anti-SARS-CoV-2 therapeutic.

One of the unexpected findings in our studies was the observation that in the absence of Beclin1 or ATG5, the SARS-CoV-2 spike protein localized in endosomes/lysosomes. Of note, however, was that the protein levels of the spike protein had not declined. Hence, although the spike localized in a LAMP2 + compartment, those vesicles had not become acidified, i.e. no protein degradation had taken place. These findings suggest that autophagic flux is required to trigger LAMP2+ vesicle acidification, and resultant spike protein degradation. The malaria drug hydroxy chloroquine has been put forward as a therapeutic which can be used to treat COVID-19 patients. Hydroxy-chloroquine acts by preventing autophagic flux, leading to a build-up of autophagosomes. Hence, theoretically, if hydroxy-chloroquine also causes translocation of the SARS-CoV-2 to LAMP2+ vesicles, a potential use for the drug against this virus may be found. i.e. a high initial dose of hydroxy-chloroquine drives spike protein into LAMP2+ vesicles concomitant with abolition of autophagic flux. Following removal and wash out of the drug, autophagic flux begins again, LAMP2+ vesicles containing spike protein acidify, and the spike protein is degraded. Of note, however, are findings
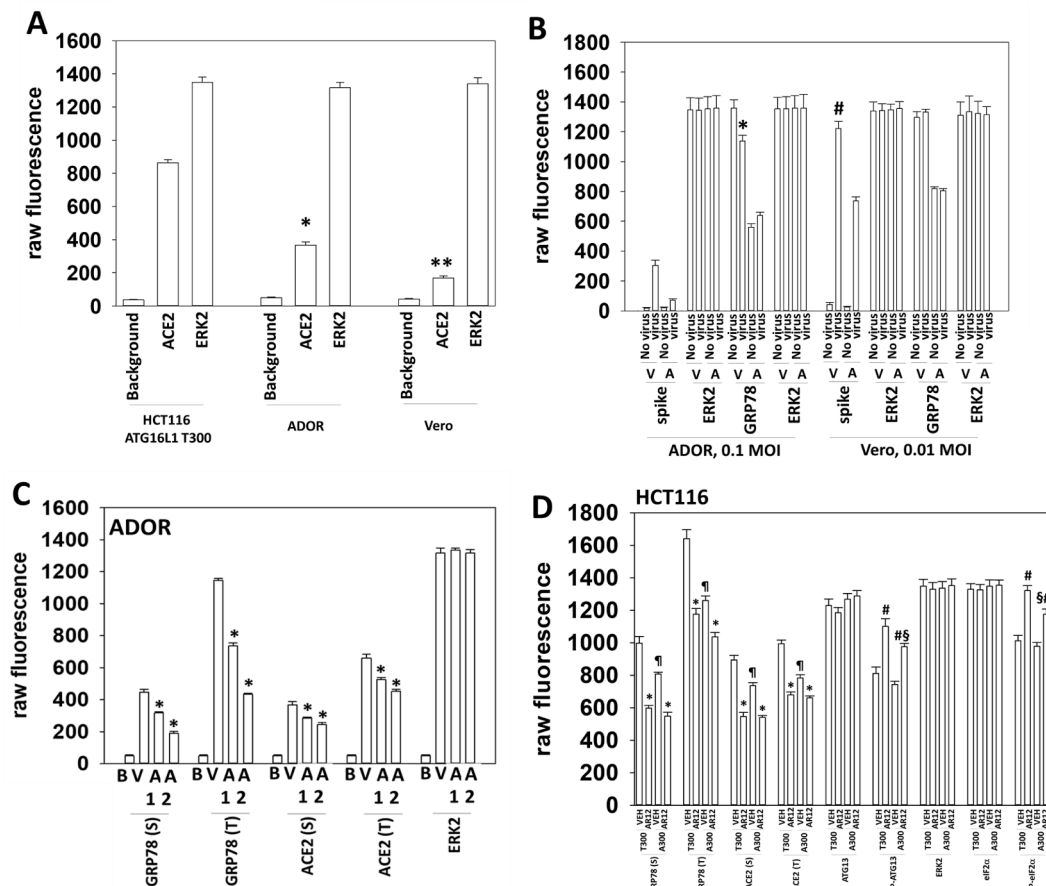
Fig. 9. HCT116 ATG16L1 T300 cells express greater amounts of GRP78 and ACE2 compared to cells expressing ATG16L1 A300 A. Vero, ADOR and HCT116 ATG16L1 T300 cells were plated and 24 h after plating, fixed and stained. Fixed cells were subjected to in-cell western blotting as described in the Methods to determine the expression of the indicated proteins (n = 3 independent studies ±SD). B. ADOR and Vero cells were treated with vehicle control or with AR12 (2 μM) and 6 h later infected with SARS-CoV-2 (0.1 MOI, 0.01 MOI). Cells were fixed in place 24 h after infection. Fixed cells were subjected to in-cell western blotting as described in the Methods to determine the expression of the indicated proteins (n = 3 independent studies ±SD). * $p < 0.05$ less than corresponding value without virus infection; # $p < 0.05$ greater than corresponding value in ADOR cells. C. ADOR cells were treated with vehicle control or with AR12 (1 μM, 2 μM). Cells were fixed in place after 6 h. Fixed cells were subjected to in-cell western blotting as described in the Methods to determine the expression of the indicated proteins (n = 3 independent studies ±SD). * $p < 0.05$ less than vehicle control. D. HCT116 ATG16L1 T300 and HCT116 ATG16L1 A300 cells were treated with vehicle control or with AR12 (2 μM). Cells were fixed in place after 6 h. Fixed cells were subjected to in-cell western blotting as described in the Methods to determine the expression and phosphorylation of the indicated proteins (n = 3 independent studies ±SD). * $p < 0.05$ less than vehicle control; ¶ $p < 0.05$ less than corresponding value in T300 cells; # $p < 0.05$ greater than vehicle control; § $p < 0.05$ less than corresponding stimulated value in T300 cells.

that hydroxy-chloroquine use is not beneficial in severely infected patients [26]. Studies beyond the scope of this manuscript will be required to confirm or refute this hypothesis.

In prior studies in the oncology field we have shown that eIF2α phosphorylation is causal in the increased expression of Beclin1 and ATG5 [5,6,15]. Those proteins were, in turn, essential for the formation of autophagosomes. Knock down of eIF2α, Beclin1 or ATG5 prevented AR12 from reducing spike protein expression. Thus, catalytic inhibition of GRP78 by AR12 leads to increased eIF2α phosphorylation which enhances Beclin1 and ATG5 expression, which promotes autophagosome formation leading to the degradation of GRP78 and spike protein.

There are relatively few biomarkers that can be used to define altered biology between different populations of humans. One such biomarker is ATG16L1 [17–22]. In our oncology studies, expression of the isoform most commonly found in African Americans, ATG16L1 T300, predicted for enhanced tumor cell killing when treating the cells with agents that utilize autophagosome formation as a component of their killing mechanism [14]. However, drug combination treatments such as gemcitabine and paclitaxel, as used to treat pancreatic cancer, utilize autophagy as a survival mechanism; African Americans respond less effectively to this drug combination than European Americans [27,28].

We discovered that cells homozygous for ATG16L1 T300 expressed approximately 20% more of the SARS-CoV-2 receptor ACE2, as well as approximately 25% higher levels of GRP78. These findings would predict for greater infectivity comparing cells expressing the T300 isoform to cells expressing the A300 isoform. However, cells expressing the A300 isoform were less capable of causing ATG13 and eIF2α phosphorylation. Clinical samples from colorectal cancer patients homozygous for ATG16L1 A300 had elevated expression of inducible type I interferons [12]. In HCT116 ATG16L1 A300 cells, the basal production of type I interferons also was enhanced, and the cells had an increased sensitivity to the double stranded RNA mimic poly (I:C) via a mitochondrial antiviral signaling (MAVS) pathway [21]. Zika virus down-regulates ATG16L1 expression and for Sindbis virus loss of ATG16L1 expression is associated with reduced eIF2α phosphorylation and viral protein synthesis [29,30]. The anti-viral activity of interferon γ also required ATG16L1 expression, with the ATG5-ATG12/ATG16L1 complex being required for norovirus to form its replication complex [31]. Enhancing our understanding of GRP78 in SARS-CoV-2 replication and understanding the role of additional chaperone proteins, e.g. HSP90 and HSP70, ATG16L1 isoform expression and type I interferon production in the life cycle and biology of SARS-CoV-2 will require detailed studies
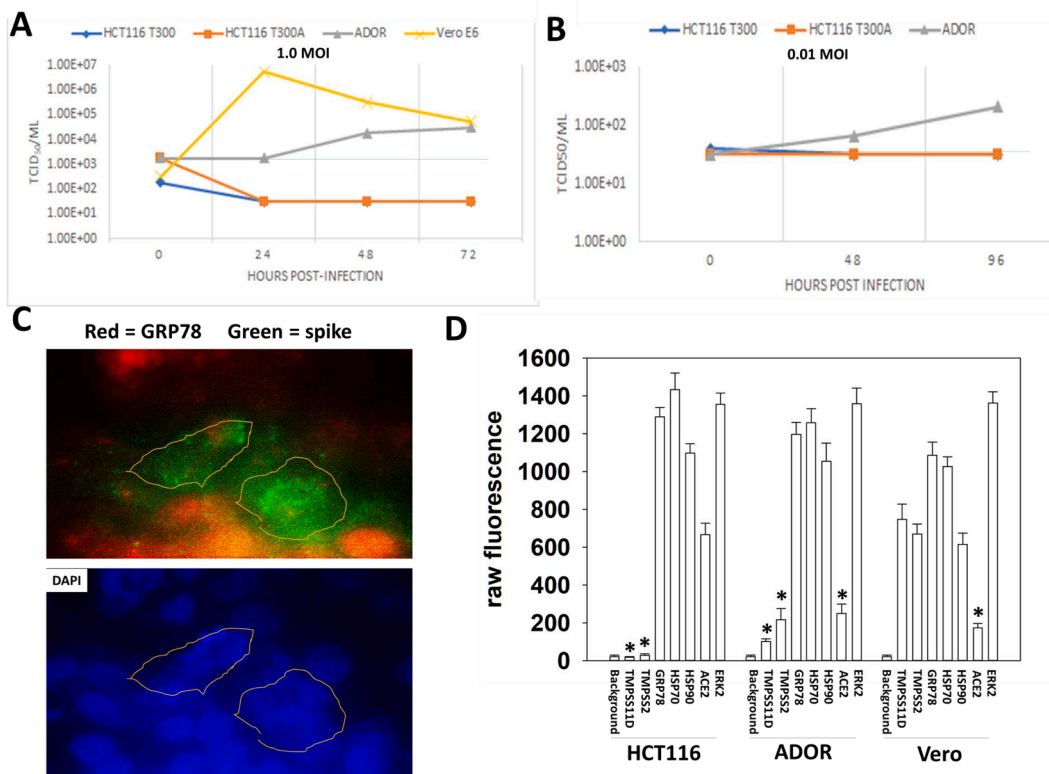
Fig. 10. The weak infectivity of ADOR cells is associated with reduced TMPRSS2 and TMPRSS11D expression. A. and B. Vero, ADOR and HCT116 cells were infected with SARS-CoV-2 (1.0 MOI, 0.01 MOI) and the media collected 24 h, 48 h and 96 h after infection. The media was diluted 1:10, with repeated 1:10 dilutions using the Reed-Muench method. Vero cells were afterwards infected with the media, and 72 h later the media was removed from the cells and TCID50/ml values determined. C. ADOR cells were infected with SARS-CoV-2 and fixed 24 h after infection. Staining was performed to determine the localization of virus spike protein, GRP78 and nuclear DNA. A representative image is presented. D. Vero and ADOR were plated and 24 h after plating, fixed and stained. Fixed cells were subjected to in-cell western blotting as described in the Methods to determine the expression of the indicated proteins (n = 3 independent studies ±SD). * $p < 0.05$ less than corresponding values in Vero cells.
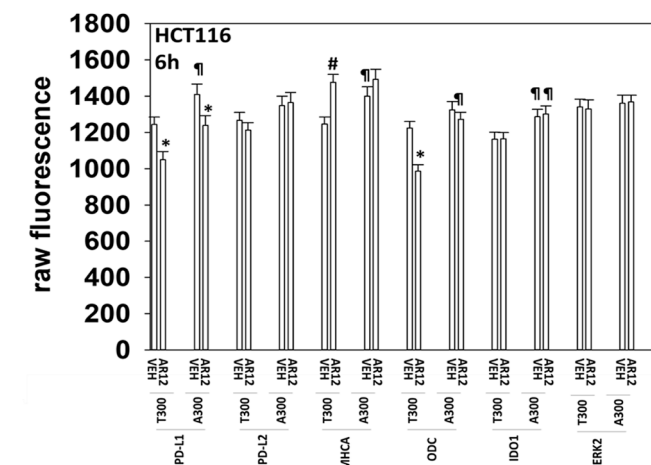
Fig. 11. AR12 reduces the expression of PD-L1 and increases the expression of MHCA. HCT116 ATG16L1 T300 and A300 cells were treated with vehicle control or with AR12 (2 µM). Cells were fixed in place after 6 h. Fixed cells were subjected to in-cell western blotting as described in the Methods to determine the expression of the indicated proteins (n = 3 independent studies ±SD). * $p < 0.05$ less than vehicle control: # $p < 0.05$ greater than vehicle control; ¶ $p < 0.05$ greater than corresponding value in T300 cells.

beyond the scope of this manuscript [32].

CRediT authorship contribution statement

Writing - review and editing.

Declaration of Competing Interest

Drs. Dent, Booth, Poklepovic and Rayner are owners in the company C19 Therapeutics; the company was formed to attract investors to fund synthesis of GMP AR12 for use in the clinic.

References

[1] G. Zhu, A.S. Lee, Role of the unfolded protein response, GRP78 and GRP94 in organ homeostasis: UPR AND GRPs REGULATE ORGAN HOMEOSTASIS, J. Cell. Physiol. 230 (7) (2015) 1413–1420.

[2] T.G. Lewy, J.M. Grabowski, M.E. Bloom, BiP: master regulator of the unfolded protein response and crucial factor in flavivirus biology, Yale J Biol Med. 90 (2017) 291–300.

[3] L. Booth, S.C. Cazanave, H.A. Hamed, A. Yacoub, B. Ogretmen, C.-S. Chen, S. Grant, P. Dent, OSU-03012 suppresses GRP78/BiP expression that causes PERK-dependent increases in tumor cell killing, Cancer Biol. Ther. 13 (4) (2012) 224–236.

[4] L. Booth, J.L. Roberts, D.R. Cash, S. Tavallai, S. Jean, A. Fidanza, T. Cruz-Luna, P. Siembida, K.A. Cycon, C.N. Cornelissen, P. Dent, GRP78/BiP/HSPA5/Dna K is a universal therapeutic target for human disease: AR-12 AND VIAGRA, J. Cell. Physiol. 230 (7) (2015) 1661–1676.

[5] L. Booth, J.L. Roberts, N. Cruickshanks, S. Grant, A. Poklepovic, P. Dent, Regulation of OSU-03012 toxicity by ER stress proteins and ER stress-inducing drugs, Mol. Cancer Ther. 13 (10) (2014) 2384–2398.

[6] L. Booth, J.L. Roberts, M. Tavallai, A. Nourbakhsh, J. Chuckalovcak, J. Carter, A. Poklepovic, P. Dent, OSU-03012 and viagra treatment inhibits the activity of multiple chaperone proteins and disrupts the blood-brain barrier: implications for anti-cancer therapies: AR-12 AND VIAGRA, J. Cell. Physiol. 230 (8) (2015) 1982–1998.

[7] J.L. Roberts, M. Tavallai, A. Nourbakhsh, A. Fidanza, T. Cruz-Luna, E. Smith, P. Siembida, P. Plamondon, K.A. Cycon, C.D. Doern, L. Booth, P. Dent, GRP78/Dna K is a target for nexavar/stivarga/votrient in the treatment of human malignancies, viral infections and bacterial diseases: SORAFENIB, REGORAFENIB, AND PAZOPANIB, J. Cell. Physiol. 230 (10) (2015) 2552–2578.

[8] L. Booth, J.L. Roberts, H. Ecroyd, S.R. Tritsch, S. Bavari, S.P. Reid, S. Proniuk, A. Zukiwski, A. Jacob, C.S. Sepúlveda, F. Giovannoni, C.C. García, E. Damonte, J. González-Gallego, M.J. Tuñón, P. Dent, AR-12 Inhibits multiple chaperones concomitant with stimulating autophagosome formation collectively preventing virus replication: CHAPERONES, AR12 AND VIRUSES, J. Cell. Physiol. 231 (10) (2016) 2286–2302.

[9] L. Booth, B. Shuch, T. Albers, J.L. Roberts, M. Tavallai, S. Proniuk, A. Zukiwski, D. Wang, C.-S. Chen, D. Bottaro, H. Ecroyd, I.O. Lebedyeva, P. Dent, Multi-kinase inhibitors can associate with heat shock proteins through their NH2-termini by which they suppress chaperone function, Oncotarget 7 (11) (2016) 12975–12996.

[10] H.-H. Chen, C.-C. Chen, Y.-S. Lin, P.-C. Chang, Z.-Y. Lu, C.-F. Lin, C.-L. Chen, C.-P. Chang, AR-12 suppresses dengue virus replication by down-regulation of PI3K/AKT and GRP78, Antiviral Res. 142 (2017) 158–168.

[11] J.-W. Chan, Z. Zhu, H. Chu, S. Yuan, K.-H. Chik, C.-S. Chan, V.-M. Poon, C.-Y. Yip, X.i. Zhang, J.-L. Tsang, Z. Zou, K.-M. Tee, H. Shuai, G. Lu, K.-Y. Yuen, The celecoxib derivative kinase inhibitor AR-12 (OSU-03012) inhibits Zika virus via down-regulation of the PI3K/Akt pathway and protects Zika virus-infected A129 mice: a host-targeting treatment strategy, Antiviral Res. 160 (2018) 38–47.

[12] W.A. Grimm, J.S. Messer, S.F. Murphy, T. Nero, J.P. Lodolce, C.R. Weber, M.F. Logsdon, S. Bartulis, B.E. Sylvester, A. Springer, U. Dougherty, T.B. Niewold, S.S. Kupfer, N. Ellis, D. Huo, M. Bissonnette, D.L. Boone, The Thr300Ala variant in ATG16L1 is associated with improved survival in human colorectal cancer and enhanced production of type I interferon, Gut 65 (3) (2016) 456–464.

[13] L.J. Reed, H. Muench, A simple method for estimating fifty percent endpoints, Am J Hyg. 27 (1938) 493–497.

[14] P. Dent, L. Booth, A. Poklepovic, J. Martinez, D.V. Hoff, J.F. Hancock, Neratinib degrades MST4 via autophagy that reduces membrane stiffness and is essential for the inactivation of PI3K, ERK1/2, and YAP/TAZ signaling, J Cell Physiol. (2020 Jan 8), https://doi.org/10.1002/jcp.29443.

[15] P. Dent, L. Booth, J.L. Roberts, J. Liu, A. Poklepovic, A.S. Lalani, D. Tuveson, J. Martinez, J.F. Hancock, Neratinib inhibits Hippo/YAP signaling, reduces mutant K-RAS expression, and kills pancreatic and blood cancer cells, Oncogene 38 (2019) 5890–5904.

[16] J. Martinez, R.K. Malireddi, Q. Lu, L.D. Cunha, S. Pelletier, S. Gingras, R. Orchard, J.L. Guan, H. Tan, J. Peng, T.D. Kanneganti, H.W. Virgin, D.R. Green, Molecular characterization of LC3-associated phagocytosis reveals distinct roles for Rubicon, NOX2 and autophagy proteins, Nat. Cell Biol. 17 (2015) 893–906.

[17] M. Varma, M. Kadoki, A. Lefkovith, K.L. Conway, K. Gao, V. Mohanan, B.K. Tusi, D.B. Graham, I.J. Latorre, A.C. Tolonen, B. Khor, A. Ng, R.J. Xavier, Cell Type– and Stimulation-Dependent Transcriptional Programs Regulated by Atg16L1 and Its Crohn's Disease Risk Variant T300A, J.I. 205 (2) (2020) 414–424.

[18] M.H. Wang, T. Okazaki, S. Kugathasan, J.H. Cho, K.L. Isaacs, J.D. Lewis, et al., Contribution of higher risk genes and European admixture to Crohn's disease in African Americans, Inflamm Bowel Dis. 18 (2012) 2277–2287.

[19] S. Lavoie, K.L. Conway, K.G. Lassen, H.B. Jijon, H. Pan, E. Chun, et al., The Crohn's disease polymorphism, ATG16L1 T300A, alters the gut microbiota and enhances the local Th1/Th17 response, eLife. 8 (2019) e39982.

[20] M. Sadaghian Sadabad, A. Regeling, M.C. de Goffau, T. Blokzijl, R.K. Weersma, J. Penders, K.N. Faber, H.J.M. Harmsen, G. Dijkstra, The ATG16L1–T300A allele impairs clearance of pathosymbionts in the inflamed ileal mucosa of Crohn's disease patients, Gut 64 (10) (2015) 1546–1552.

[21] K.G. Lassen, P. Kuballa, K.L. Conway, K.K. Patel, C.E. Becker, J.M. Peloquin, E.J. Villablanca, J.M. Norman, T.-C. Liu, R.J. Heath, M.L. Becker, L. Fagbami, H. Horn, J. Mercer, O.H. Yilmaz, J.D. Jaffe, A.F. Shamji, A.K. Bhan, S.A. Carr, M.J. Daly, H.W. Virgin, S.L. Schreiber, T.S. Stappenbeck, R.J. Xavier, Atg16L1 T300A variant decreases selective autophagy resulting in altered cytokine signaling and decreased antibacterial defense, Proc. Natl. Acad. Sci. 111 (21) (2014) 7741–7746.

[22] Q.-X. Li, X. Zhou, T.-T. Huang, Y. Tang, B.o. Liu, P. Peng, L.i. Sun, Y.-H. Wang, X.-L. Yuan, The Thr300Ala variant of ATG16L1 is associated with decreased risk of brain metastasis in patients with non-small cell lung cancer, Autophagy 13 (6) (2017) 1053–1063.

[23] A. Shulla, T. Heald-Sargent, G. Subramanya, J. Zhao, S. Perlman, T. Gallagher, A transmembrane serine protease is linked to the severe acute respiratory syndrome coronavirus receptor and activates virus entry, J. Virol. 85 (2011) 873–882.

[24] T. Meng, H. Cao, H. Zhang, Z. Kang, D. Xu, H. Gong, J. Wang, Z. Li, X. Cui, H. Xu, H. Wei, X. Pan, R. Zhu, J. Xiao, W. Zhou, L. Cheng, J. Liu, The insert sequence in SARS-CoV-2 enhances spike protein cleavage by TMPRSS. bioRxiv 2020: doi: https://doi.org/10.1101/2020.02.08.926006.

[25] A.E. Renteria, L. Endam Mfuna, D. Adam, A. Filali-Mouhim, A. Maniakas, S. Rousseau, E. Brochiero, S. Gallo, M. Desrosiers, Azithromycin downregulates gene expression of il-1β and pathways involving TMPRSS2 and TMPRSS11D required by SARS-CoV-2, Am J Respir Cell Mol Biol. (2020 Aug 28), https://doi.org/10.1165/rcmb.2020-0285LE.

[26] N. Hussain, E. Chung, J. Heyl, et al., A Meta-Analysis on the Effects of Hydroxychloroquine on COVID-19, Cureus 12 (2020) e10005. doi:10.7759/cureus.10005.

[27] M.-C. Yang, H.-C. Wang, Y.-C. Hou, H.-L. Tung, T.-J. Chiu, Y.-S. Shan, Blockade of autophagy reduces pancreatic cancer stem cell activity and potentiates the tumoricidal effect of gemcitabine, Mol. Cancer 14 (2015), https://doi.org/10.1186/s12943-015-0449-3.

[28] H.J. Zeh, N. Bahary, B.A. Boone, A.D. Singhi, J.L. Miller-Ocuin, D.P. Normolle, A.H. Zureikat, M.E. Hogg, D.L. Bartlett, K.K. Lee, A. Tsung, J.W. Marsh, P. Murthy, D. Tang, N. Seiser, R.K. Amaravadi, V. Espina, L. Liotta, M.T. Lotze, A Randomized Phase II Preoperative Study of Autophagy Inhibition with High-Dose Hydroxychloroquine and Gemcitabine/Nab-Paclitaxel in Pancreatic Cancer Patients, Clin Cancer Res 26 (2020).

[29] M. Jefferson, B. Bone, J.L. Buck, P.P. Powell, The autophagy protein ATG16L1 is required for sindbis virus-induced eif2α phosphorylation and stress granule formation, Viruses 12 (2019) 39.

[30] M.E. Hill, A. Kumar, J.A. Wells, T.C. Hobman, O. Julien, J.A. Hardy, The unique cofactor region of zika virus NS2B–NS3 protease facilitates cleavage of key host proteins, ACS Chem. Biol. 13 (9) (2018) 2398–2405.

[31] S. Hwang, N. Maloney, S. Bruinsma, G. Goel, E. Duan, L. Zhang, B. Shrestha, M. Diamond, A. Dani, S. Sosnovtsev, K. Green, C. Lopez-Otin, R. Xavier, L. Thackray, H. Virgin, Nondegradative role of Atg5-Atg12/ Atg16L1 autophagy protein complex in antiviral activity of interferon gamma, Cell Host Microbe 11 (2012) 397–409.

[32] D.P. Ha, R.V. Krieken, A.J. Carlos, A.S. Lee, The stress-inducible molecular chaperone GRP78 as potential therapeutic target for coronavirus infection, J. Infect. 15 (2020) 50.